Light Delivery over Extended Time Periods Enhances the Effectiveness of Photodynamic Therapy

Mukund Seshadri,[1,2] David A. Bellnier,[1] Lurine A. Vaughan,[1] Joseph A. Spernyak,[2] Richard Mazurchuk,[2] Thomas H. Foster,[3] and Barbara W. Henderson[1]

Abstract

Purpose: The rate of energy delivery is a principal factor determining the biological consequences of photodynamic therapy (PDT). In contrast to conventional high-irradiance treatments, recent preclinical and clinical studies have focused on low-irradiance schemes. The objective of this study was to investigate the relationship between irradiance, photosensitizer dose, and PDT dose with regard to treatment outcome and tumor oxygenation in a rat tumor model.

Experimental Design: Using the photosensitizer HPPH (2-[1-hexyloxyethyl]-2-devinyl pyropheophorbide), a wide range of PDT doses that included clinically relevant photosensitizer concentrations was evaluated. Magnetic resonance imaging and oxygen tension measurements were done along with the Evans blue exclusion assay to assess vascular response, oxygenation status, and tumor necrosis.

Results: In contrast to high-incident laser power (150 mW), low-power regimens (7 mW) yielded effective tumor destruction. This was largely independent of PDT dose (drug-light product), with up to 30-fold differences in photosensitizer dose and 15-fold differences in drug-light product. For all drug-light products, the duration of light treatment positively influenced tumor response. Regimens using treatment times of 120 to 240 min showed marked reduction in signal intensity in T2-weighted magnetic resonance images at both low (0.1 mg/kg) and high (3 mg/kg) drug doses compared with short-duration (6-11 min) regimens. Significantly greater reductions in pO_2 were observed with extended exposures, which persisted after completion of treatment.

Conclusions: These results confirm the benefit of prolonged light exposure, identify vascular response as a major contributor, and suggest that duration of light treatment (time) may be an important new treatment variable.

Recent developments in photodynamic therapy (PDT), the activation of tumor-localized photosensitizer by light, have focused on prolonged, low-irradiance (incident fluence rate) light delivery compared with conventional rapid, high-irradiance light treatment (1–3). Treatment schemes based on long irradiation times have also been used in clinical trials of newer photosensitizers (4). The rate of energy delivery has long been recognized as the principal factor determining the biological consequences of treatment modalities that require absorption of energy in tissue. For ionizing radiation, especially with X-rays or γ-rays, lowering the irradiation dose rate usually results in reduced effectiveness, a phenomenon largely explained by the repair of sublethal damage during prolonged irradiation (5). A similar phenomenon is observed with PDT at extremely low dose rates (6–8). However, within a clinically relevant range, relatively lower irradiances have been shown to lead to enhanced antitumor activity of PDT (9–12). The mechanistic basis for the superiority of low-fluence rate PDT has been interpreted primarily in relation to conservation of tissue oxygenation. Oxygen is critical for photodynamic activity because the cytotoxic agent, singlet oxygen ($^1O_2$), arises as a result of the energy transfer from the excited photosensitizer to ground state oxygen ($^3O_2$) residing in the tissue being treated (13). High-fluence rate PDT can lead to treatment-limiting deficits in available oxygen if the high rate of $^1O_2$ generation outpaces the resupply of oxygen through the blood. This photodynamic oxygen consumption (14, 15) has been well documented in both preclinical and clinical studies (11, 16–19). The dominant determinants of the rate of photochemical oxygen depletion are (*a*) photosensitizer concentration in tissue, (*b*) absorption coefficient of the photosensitizer, (*c*) fluence rate of light, and (*d*) tissue oxygenation through perfusion. These variables can change during light delivery, such as reduction in photosensitizer concentration through photobleaching (20) or alterations in vascular function (21). Studies in a murine model have shown that changes in vascular

Authors' Affiliations: [1]Department of Cell Stress Biology and Photodynamic Therapy Center and [2]Preclinical Imaging Resource, Roswell Park Cancer Institute, Buffalo, New York and [3]Department of Imaging Sciences, University of Rochester, Rochester, New York

Received 10/22/07; revised 12/21/07; accepted 1/18/08.

Grant support: NIH grants CA42278 (B.W. Henderson) and CA55791 (A.R. Oseroff). This work also received support from Light Sciences Corp. and used core facilities supported in part by Roswell Park Cancer Institute's National Cancer Institute – funded Cancer Center Support grant CA16056.

The costs of publication of this article were defrayed in part by the payment of page charges. This article must therefore be hereby marked *advertisement* in accordance with 18 U.S.C. Section 1734 solely to indicate this fact.

Requests for reprints: Barbara W. Henderson, Photodynamic Therapy Center, Roswell Park Cancer Institute, Elm and Carlton Streets, Buffalo, NY 14263. Phone: 716-845-4429; Fax: 716-845-8920; E-mail: Barbara.Henderson@roswellpark.org.

doi:10.1158/1078-0432.CCR-07-4705

perfusion can also be fluence rate dependent, albeit involving the vessels of the normal skin rather than the tumor (22).

Although the principle of fluence rate–dependent modulation of PDT efficacy is now well supported, a large discrepancy exists between preclinical and clinical studies exploring this modulation, with regard to photosensitizer concentration in tissue. Although murine studies using Photofrin have reported tumor concentrations of ~10 μg/g (11), such levels have not been achieved in human tumors within the range of clinically acceptable Photofrin doses [e.g., a mean of ~1.5 μg/g in mesothelioma after a 2 mg/kg drug dose (23); a mean of ~3 μg/g in i.p. carcinomatosis and sarcomatosis lesions after a 2.4 mg/kg drug dose, with 10-fold variabilities (24); and a median of 0.5 μg/g in basal cell carcinomas after a 1 mg/kg drug dose (17, 25)].

Given the importance of photosensitizer concentration in tissue as a determinant for tumor oxygenation during PDT, in the present study, we aimed to explore a large dose-response surface that includes clinically relevant dose variables. Using magnetic resonance imaging (MRI) as a noninvasive tool to assess the vascular response and tumor oxygenation status as well as direct oxygen tension measurements and tumor response determinations, we confirm the benefit of prolonged light exposure, identify the vascular response as a major contributor to this beneficial outcome, and suggest that duration of light delivery (time) may be an important new treatment variable.

Materials and Methods

Animals and tumor system. Female Fischer 344/N rats (body weight, 150-180 g), 8 to 12 wk of age, were obtained from Harlan Sprague Dawley, Inc. The chemically induced Ward colon carcinoma (WCT) was implanted s.c. on the shoulder or hind flank using a trocar as described previously (26). Tumors were used for experiments when they reached ~2 to 2.5 cm in diameter (~17 d after implantation) and ~1 cm in depth. All procedures were carried out in accordance with protocols approved by the Institutional Animal Care and Use Committee at Roswell Park Cancer Institute.

Photosensitizer. Clinical-grade, pyrogen-free HPPH (2-[1-hexyloxyethyl]-2-devinyl pyropheophorbide-a) was obtained from the Roswell Park Pharmacy and reconstituted to 0.4 mmol/L in pyrogen-free 5% dextrose (D5W; Baxter Corp.) containing 2% ethanol and 0.1% Tween (27, 28). HPPH was given via tail vein injection at 0.033, 0.1, 0.3, 1.0, and 3.0 mg/kg.

Determination of HPPH concentration in tumors. [^{14}C]HPPH was prepared as described earlier (29). [^{14}C]HPPH was given to rats through a lateral tail vein injection. Approximately 24 h after injection, the rats were euthanized and tumors were excised and cut into small sections so that each sample weighed <200 mg. Specimens were transferred to a scintillation vial containing 1 mL Solvable (Packard Bioscience) tissue solubilizer and heated overnight at 53°C as described previously (30). Samples were decolorized with 30% H_2O_2, as required, followed by addition of 15 mL Ultima Gold scintillation mixture (Perkin-Elmer) and counting with a Beckman LS 6500 liquid scintillation counter (Beckman Coulter).

In vivo *PDT treatment.* Twenty-four hours after photosensitizer administration, hair was removed by shaving from the treatment sites and from tumors that served as unilluminated controls. Due to the frequently prolonged light exposure times, which necessitated free movement of the animals, rats were fitted with an infusion harness (Covance Infusion Harness, Harvard Apparatus) to which the optical light delivery fiber was attached. A 400-μm flat-cut fiber was threaded through and fixed at the infusion port so that the fiber tip was within 1 mm of the tumor surface. Such a light delivery setup closely resembles certain clinical tumor treatments. The light source consisted of a dye laser (375; Spectra-Physics) pumped by an argon ion laser (either 171 or 2080; Spectra-Physics). The dye laser, using 4-dicyanomethylene-2-methyl-6-*p*-dimethylaminostyryl-4H-pyran (DCM) dye (Exciton), was tuned to 665 nm. The power output from the fiber was set to range from 3 to 150 mW. Tumor temperatures were measured in a set of control experiments by means of an Omega HYP-0 30-gauge needle thermocouple (Omega Engineering, Inc.) inserted at a tumor depth of ~3 to 5 mm from the surface. At the highest laser power of 150 mW, the largest temperature increase registered was 2.6°C above baseline, and the highest temperature measured was 35.4°C. Any temperature increase occurred within the first 5 min of light exposure, after which the temperature remained stable. No temperature increases were observed at laser powers of 50 mW or below. For MRI studies, the output from the laser was directed into the scanner using an optical fiber to allow real-time image acquisition during light treatment.

Assessment of tumor response. Animals were given Evans blue [350 μL i.v. 5% (w/v) in saline] 72 h after completion of treatment. The dye distributes throughout viable tissue with functional vasculature but is excluded from necrotic tissue that is devoid of intact blood vessels. Immediately after dye administration, the animals were euthanized with CO_2 and the tumors were harvested. Tumors were bisected vertically along the centerline of the light field and arranged with the cut side up alongside a ruler, and digital photographs were acquired. PDT-induced tumor necrosis was clearly visible by its light color due to the exclusion of Evans blue, whereas viable tissue was stained dark blue. Areas of Evans blue exclusion corresponded with areas of tumor necrosis on histologic examination. Occasional small areas of spontaneous necrosis had a dark brown appearance and were easily distinguishable from PDT-generated necrosis. Photographs of tumors were analyzed using the Zeiss AxioVision LE Rel. 4.1 software (Carl Zeiss MicroImaging, Inc.). The area of PDT necrosis was precisely (0.1 mm ± 10%) outlined and the number of pixels was converted to cm^2 using the ruler image as a guide. The accuracy of the necrosis measurements was validated by two independent operators. According to the two-tailed *t* test, the *P* value for these measurements was 0.7594, indicating that the measurements obtained from the two independent operations were not significantly different.

Computer simulation of $^3O_2$ and $^1O_2$ distribution in tumor tissue during PDT. Computer software (PDT molecular oxygen depletion model, PDT MODeM), developed by Henning et al. (31), was used to compute the potential effects of fluence rate on $^3O_2$ and $^1O_2$ distribution throughout the intercapillary space during PDT. Reaction variables (molecular weight, 636; ε = 50,000 cm^{-1} mol/L^{-1}; λ = 665; Φ_T = 0.55; tissue metabolic O_2 consumption rate = 1.7 μmol/L/s; intercapillary distance = 300 μm; all other reaction variables were assumed as for porfimer sodium) were set as described previously (11), with the exception of HPPH tumor concentrations, which were based on the measured values using [^{14}C]HPPH.

Blood oxygenation level–dependent functional MRI of tumor oxygenation. To determine fluence rate effects on tumor oxygenation during light treatment, noninvasive functional MRI (fMRI) sensitive to blood oxygenation level–dependent (BOLD) contrast (32) was done. BOLD fMRI uses differences in spin-spin (T2) relaxation times that arise from field gradients in the vicinity of blood vessels carrying deoxyhemoglobin versus oxyhemoglobin (32). Images were acquired on a 4.7-T/33-cm horizontal bore magnet (GE NMR Instruments) incorporating AVANCE digital electronics (Bruker Biospec with ParaVision 3.0.2; Bruker Medical) and a 72-mm quadrature rat transceiver coil. Before magnetic resonance acquisitions, tumor-bearing rats (n = 3-4/treatment group) were anesthetized using i.p. injection of ketamine-xylazine mixture (50:2.2 mg/mL) at a dose volume of 1.8 mL/kg, secured in a plastic carrier tube, and positioned in the scanner. A circulating warm water bath (39°C, Neslab RTE-221) was used to maintain the body temperature of animals during image acquisition. Respiratory rates of animals during image acquisition were monitored using a small animal monitoring system (model 1025; SA Instruments,

Inc.) and anesthesia was maintained using low concentrations of isoflurane as required. A series of T2-weighted fast spin echo acquisitions (effective time of echo period = 80.3 ms; repetition time = 2,800 ms; field of view = 8.0 cm × 6.0 cm; matrix size = 128 × 128; slice thickness = 1.25 mm; 15 slices; number of averages = 4) were acquired before, during, and after light treatment. A typical imaging protocol consisted of three sequential images acquired before illumination followed by a series of images acquired during light treatment, the number being dependent on the laser energy and incident power used, and three images were acquired after the completion of light treatment.

Image processing and analysis of MRI data were done using commercially available imaging software (Analyze PC, version 7.0; Biomedical Imaging Resource, Mayo Clinic, Rochester, MN). Functional T2 activation maps of changes in magnetic resonance signal intensity (SI) were calculated on a pixel-by-pixel basis from sequential images acquired before and during light treatment using MATLAB (version 7.0; MathWorks, Inc.) using source codes developed at Roswell Park Cancer Institute's Preclinical Imaging Resource. Activation maps representing positive and negative change were displayed using a color look-up table superimposed on corresponding anatomic images. Only pixels that showed a statistically significant ($P < 0.05$) change from baseline were reported.

Direct measurement of tumor oxygenation. Tumor oxygen measurements were obtained using the OxyLite system (Oxford Optronix). This methodology measures pO_2 by determining the O_2-dependent fluorescence lifetime of ruthenium chloride immobilized at the tip of a 250-μm fiber optic probe (33). Because the method is fluorescence based, measurements cannot be carried out during PDT light delivery due to photobleaching of the probe. Therefore, measurements were carried out in untreated control tumors and in PDT-treated tumors at different times after light exposure. Before measurement, rats were anesthetized using ketamine (50 mg/mL)-xylazine (2.2 mg/mL) mixture at a dose volume of 1.8 mL/kg. A 21-gauge needle was used to pierce the skin over the tumor and to facilitate penetration into the tumor, and the pO_2 probe was subsequently inserted to a depth of ~2 mm. The needle was then partially withdrawn, leaving the probe in place. OxyLite measures pO_2 levels at a single point of placement with the volume sampled being confined to the sensor tip. Therefore, the probe was placed at two to three points within a given tumor, with three to five individual tumors assessed for each experimental group. At least 15 values were obtained at an interval of 5 s from each tumor after the probe reading stabilized ~10 min after insertion.

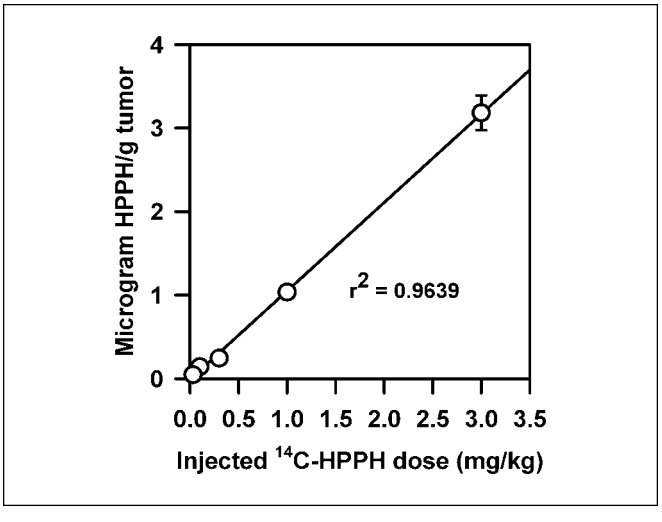

Fig. 1. Accumulation of [^{14}C]HPPH in Ward colorectal carcinomas as a function of injected dose. Tumors were harvested 24 h after HPPH administration. Points, mean of three tumors; bars, SE.

Table 1. Treatment variables

Treatment variable	Range
HPPH dose (mg/kg)	0.033-3.0
Energy (J)	50-1500
Drug-light product	5-150
Incident laser power (mW)	3-150
Length of light delivery (min)	6-1665

Statistical analysis. Statistical analysis (GraphPad Prism, version 4.00; GraphPad Software) was done by comparing the treatment groups with untreated controls using the two-tailed t test and P values of ≤0.05 were considered statistically significant.

Results

HPPH tumor uptake is linearly related to injected HPPH dose. Photosensitizer tumor concentration is a major determinant for PDT-induced oxygen depletion and has to be known to predict oxygen-depleting or oxygen-conserving fluence rates for treatment. Measurements of HPPH tumor concentration using ^{14}C-labeled drug revealed that drug uptake was linear (regression coefficient $r^2 = 0.9639$) over a 100-fold range of injected drug doses (0.033-3.0 mg/kg; Fig. 1). The numerical values of injected drug doses given in mg/kg corresponded closely with the values of measured tumor drug concentration in μg/g tissue (i.e., 1 mg/kg HPPH resulted in ~1 μg/g HPPH in tissue).

Duration of light delivery influences PDT treatment outcome. To explore the relationship between drug dose, laser energy, laser power, and their influence on tumor destruction by PDT, 45 drug-light variable combinations (ranges listed in Table 1) were explored. PDT dose is composed of drug and light dose, which can be expressed as the drug-light product, whereby drug and light are considered reciprocal (34). Thus, tumor response should be similar as long as the drug-light product is the same. However, because the drug concentration in the tumor is a major determinant for fluence rate–dependent oxygen depletion, the fluence rate dependence of treatment outcome would be expected to be different for different drug doses/tumor concentrations. We first addressed this issue by determining the tumor response, assessed by measuring the area of necrosis under conditions of equal drug-light products achieved through reciprocal drug and light treatment conditions (3 mg/kg HPPH, 50 J; 1 mg/kg HPPH, 150 J). As expected, the area of necrosis achieved was not significantly different between the two PDT regimens, confirming drug-light reciprocity (Fig. 2). Surprisingly, the pattern of dependence on the laser power was similar at both drug doses, with the largest area of necrosis observed at 7 mW and a drop in effectiveness at 3 mW. Considering the possibility that the drug concentrations used did not sufficiently vary between the two regimens, we next analyzed conditions that used 10-fold differences in drug concentration, therefore resulting in a 10-fold difference in drug-light product. At an incident power of 7 mW, the regimens resulted in similar areas of necrosis (0.1 mg/kg, 100 J = 0.812 cm^2 ± 0.06 SE; 1.0 mg/kg, 100 J = 0.926 cm^2 ± 0.069 SE; $P = 0.223$). When the power was increased to 150 mW, both regimens were ineffective (0.1 mg/kg,

100 J = 0.027 cm^2 ± 0.01 SE; 1.0 mg/kg, 100 J = 0.176 cm^2 ± 0.098 SE; P = 0.163). At both drug doses, differences in area of necrosis between 7 and 150 mW were highly significant ($P < 0.001$).

We next considered the length of time required to deliver each of the 45 regimens. The treatment time (length of illumination) is dictated by the desired total energy and rate at which energy is delivered (power). When the area of necrosis for all drug-light products is plotted against total duration of light delivery (time), it becomes evident that increasing both drug-light product and, more prominently, the time it took to deliver a given treatment positively influenced the tumor response (Fig. 3). A treatment regimen of high PDT dose at high-incident power (indicated by the asterisk in Fig. 3; 3 mg/kg HPPH, 100 J, 150 mW) resulted in considerable tumor necrosis but at the expense of normal tissue damage, intense pain, and distress to the animal that required anesthesia during treatment. To test whether there is a lower limit of effective HPPH dose, we used regimens using 0.033 mg/kg (~0.048 μg/g tumor concentration). Minimal tumor necrosis (data not shown) was achieved with 300 J (drug-light product = 10) at 150 mW (33 min; area of necrosis = 0.13 ± 0.02 SE) and at 3 mW (1,665 min; area of necrosis = 0.19 ± 0.06 SE). These data indicate that there seems to be a threshold for effective drug dose that cannot be overcome by prolonging the light exposure.

Exploring the very low but effective range of photosensitizer doses (0.1 versus 3.0 mg/kg), a strikingly similar dependence on treatment laser power was observed (Fig. 4A). Despite a 15-fold difference in drug-light product and a 30-fold difference in injected HPPH dose and tissue concentration, Evans blue exclusion revealed that 7 mW was far superior to 150 mW ($P < 0.001$). In addition to the differences in drug dose and drug-light product, it is important to note that the treatment times varied greatly between the different regimens used [100 J at 150 mW (11 min); 100 J at 7 mW (238 min); 50 J at 150 mW (5.5 min); and 50 J at 7 mW (119 min)].

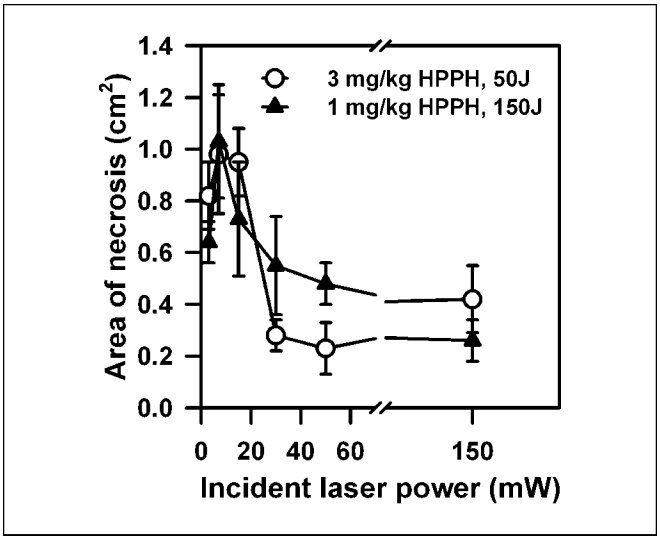

Fig. 2. Area of necrosis in Ward colorectal carcinomas as a function of incident laser power. Tumors were exposed to light 24 h after HPPH administration. Points, mean of five to eight individual rats/tumors; bars, SE.

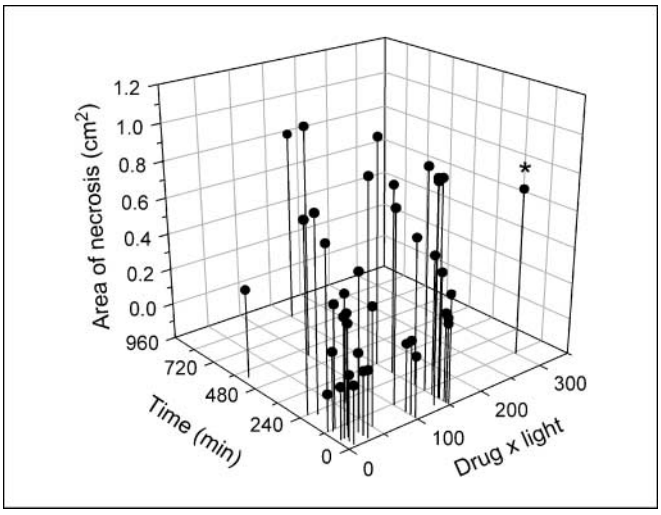

Fig. 3. Area of necrosis in Ward colorectal carcinomas as a function of drug-light product and time. For ranges in PDT variables, see Table 1. Points, mean values of three to eight individual rats/tumors.

Simulation of pO_2 and $^1O_2$ distribution during PDT can adequately explain the benefit of low fluence rate under high HPPH dose conditions but fails under low HPPH dose conditions. Under the illumination conditions used in this study, large gradients of fluence rates exist throughout the tumor depth, being high toward the tumor surface and low toward the tumor base. However, at a certain tumor depth, fluence rates of 150 or 7 mW cm^{-2} will prevail. Overall, the spectrum of fluence rates throughout the tumor will be ~20-fold greater at an incident power of 150 mW than at 7 mW. To gain some insight into the mechanisms determining the above unexpected outcome, we first turned to a simulation of tumor oxygenation as a function of fluence rate during PDT for the four different regimens shown in Fig. 4A. These computations do not take into account any possible changes in vascular oxygen supply or photobleaching of the photosensitizer during illumination. They also only reflect the situation at the certain tumor depth where the specific computed fluence rates might prevail. Changes in photosensitizer concentration over the duration of light delivery are negligible (29). We have used this approach in the past in several preclinical and clinical studies for predicting PDT-induced changes in tumor oxygenation and have been able to validate these predictions (11, 17, 35). Using the PDT molecular oxygen depletion model computer software (31) and HPPH-specific photophysical and Ward tumor HPPH concentration variables, we simulated the instantaneous steady-state distribution of $^3O_2$ (Fig. 4B) and $^1O_2$ (Fig. 4C). Figure 4B (*right*) shows the predicted oxygen distribution within the tumor, sensitized with 3 mg/kg HPPH, as a function of distance from a blood vessel at a fluence rate of 150 and 7 mW cm^{-2}. Ground state oxygen is expected to be completely depleted within a distance of 40 μm from the capillary at 150 mW cm^{-2}, whereas oxygen depletion at 7 mW cm^{-2}, although severe, only approaches anoxia at 150 μm. The corresponding simulation of $^1O_2$ distribution (Fig. 4C, *right*) predicts very high levels of singlet oxygen generated close to the capillary wall 150 mW cm^{-2} but falling rapidly to zero corresponding with the predicted lack of available ground state oxygen. In contrast, 7 mW cm^{-2} would instantaneously generate much lower levels of $^1O_2$

that would be maintained over the full distance of 150 μm (~5 pmol/L at vessel wall to ~0.7 pmol/L at 150 μm). These simulations would correctly predict a poor response for the high-fluence rate treatment because much of the tumor volume would be devoid of available oxygen during treatment and would therefore be protected from PDT damage.

A very different scenario would be expected for the low HPPH (0.1 mg/kg) dose regimen. Here, ground state oxygen depletion at a fluence rate of 150 mW cm^{-2} (Fig. 4B, *left*), although predicted to occur, is comparable with that seen with the 3 mg/kg HPPH dose at the 7 mW cm^{-2} fluence rate (Fig. 4B, *right*). At 7 mW cm^{-2} with the low drug dose, oxygenation is expected to be well maintained and comparable with levels associated with metabolic oxygen consumption. Correspondingly, instantaneous $^1O_2$ levels (Fig. 4C, *left*) throughout the distance from the capillary at 150 mW cm^{-2} are expected to be very similar (ranging from ~4 to ~1 pmol/L at distance) to those expected with the low fluence rate at the high drug dose (Fig. 4C, *right*; note difference in the scale of the *Y* axis between *left* and *right*). Despite this predicted similarity, high laser power is ineffective at low drug dose. In contrast, extremely low $^1O_2$ levels maintained throughout the distance (~0.2 pmol/L) are predicted for the low-drug dose and low-fluence rate regimen. Interestingly, despite the predicted higher levels of singlet oxygen generated over the entire intercapillary distance with 0.1 mg/kg HPPH at high versus low fluence rate, the actual high-power treatment was less effective. It should be noted that the light exposure time for the low-power treatment regimen was >20 times longer than for the high-power protocol. Taken together, the computed simulations suggest that very low levels of singlet oxygen, maintained throughout the tumor volume for prolonged periods of time, are highly effective in destroying tumor tissue.

Duration of light delivery influences tumor oxygenation as determined by noninvasive imaging. In an effort to validate the above modeling predictions and explore the mechanisms

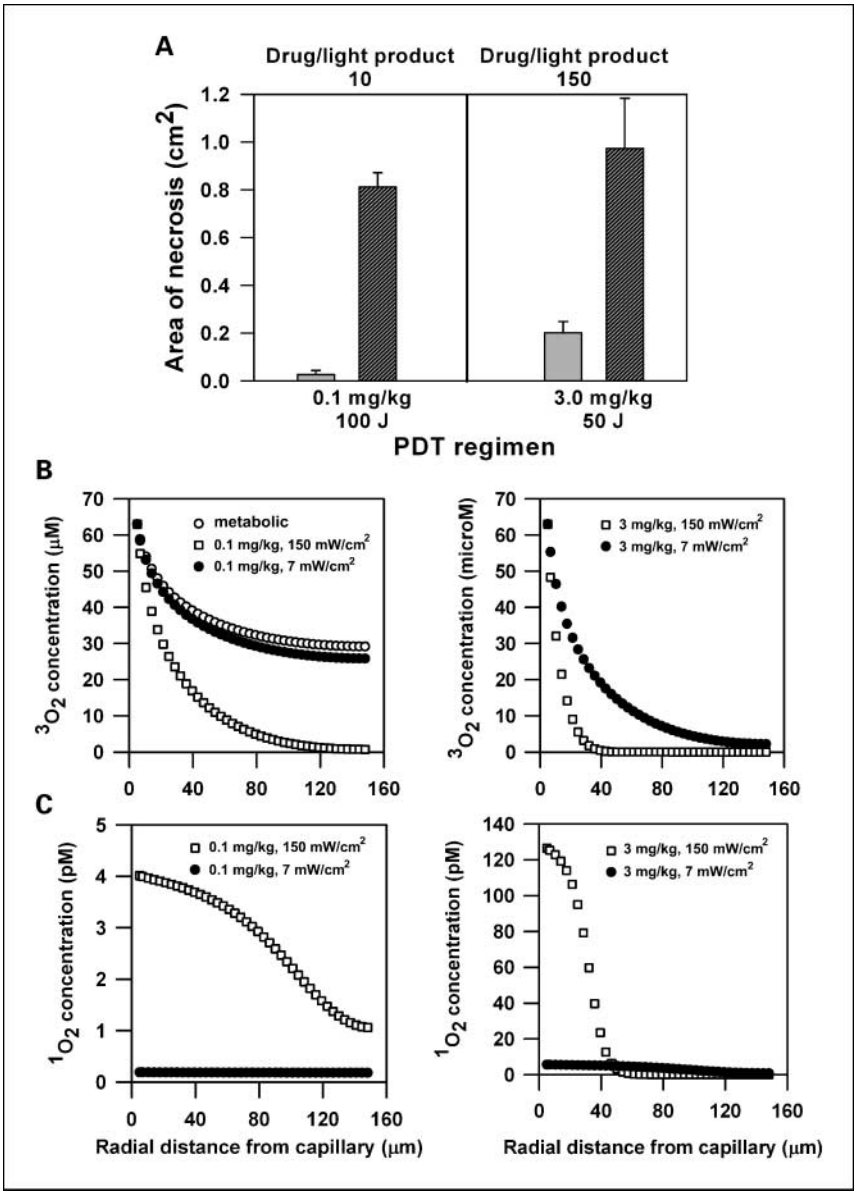

Fig. 4. Area of necrosis in Ward colorectal carcinomas as a function of drug-light product and time. *A,* area of necrosis in Ward colorectal carcinomas as a function of PDT regimen. Light columns, 150 mW incident laser power; dark columns, 7 mW incident laser power. Columns, mean of five to eight rats/tumors; bars, SE. *B,* simulated ground state oxygen distribution, plotted by PDT molecular oxygen depletion model as a function of distance from a capillary, in tumors treated with fluence rates of 7 mW cm^{-2} (*left*) and 150 mW cm^{-2} (*right*). *C,* simulated singlet oxygen distribution, plotted as above, in tumors treated with fluence rates of 7 mW cm^{-2} (*left*) and 150 mW cm^{-2} (*right*).

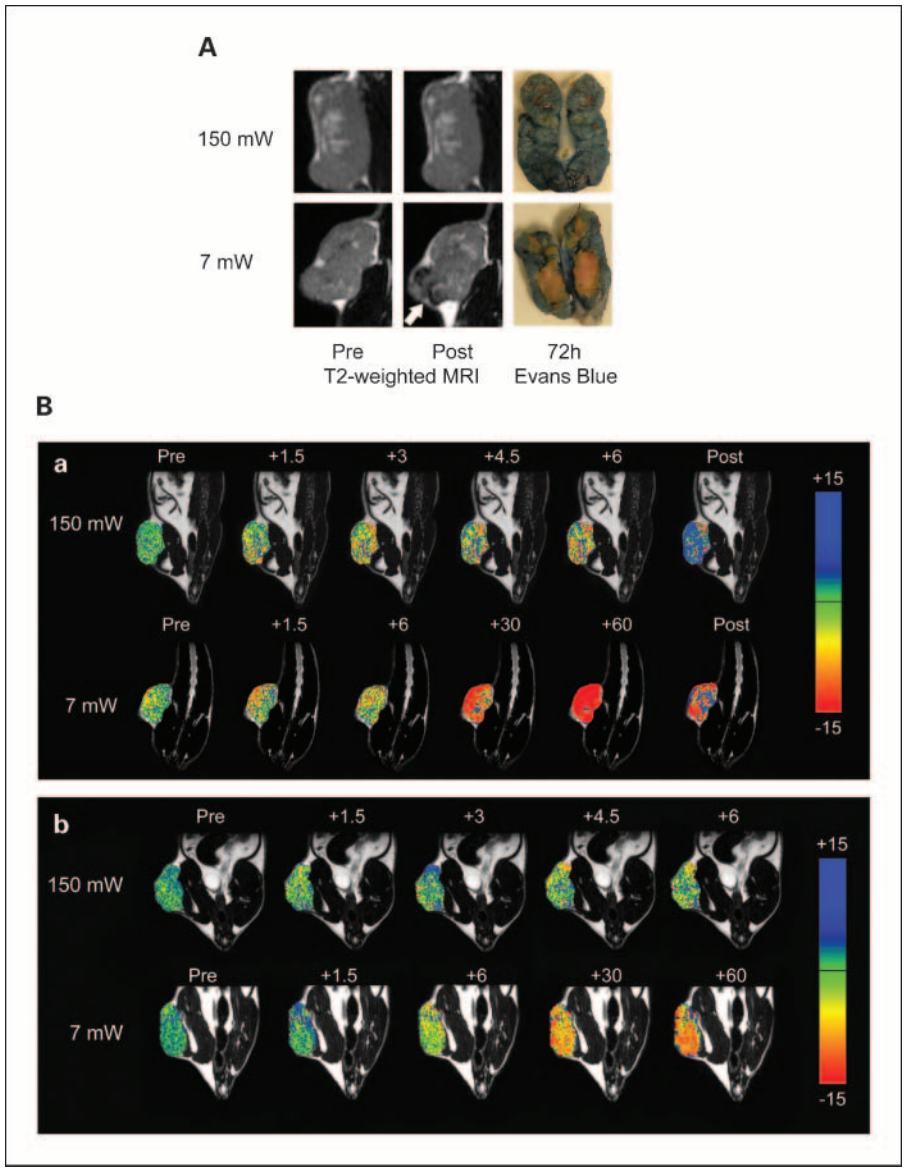

Fig. 5. T2-weighted BOLD MRI of tumor oxygenation during PDT. *A,* T2-weighted magnetic resonance images of Ward colorectal carcinomas before (*Pre*) and after (*Post*) completion of HPPH-sensitized PDT [3 mg/kg HPPH; 150 mW (*top*) or 7 mW (*bottom*)]. Corresponding digital images, following injection of Evans blue 72 h after completion of treatment, are also shown. *B,* pseudocolor-coded images of magnetic resonance SI change before (*Pre*), during (+1.5, +3, +4.5, and +6 min), and after (*Post*) PDT following injection of 3 mg/kg HPPH (*a*) or 0.1 mg/kg HPPH (*b*). Tumor illumination was carried out at 150 and 7 mW.

governing the treatment outcome, BOLD fMRI (32) was used during and after light delivery for the selected regimens for which oxygen modeling and tumor response data had been acquired.

Figure 5A depicts T2-weighted functional magnetic resonance images in the left and middle panels and images of the corresponding tumor response in the right panels. Tumors were treated with PDT at 3 mg/kg HPPH and 50 J with laser powers of 7 mW (119 min) and 150 mW (6 min), respectively. Serial T2-weighted images were acquired before commencement of light delivery and immediately after completion of light treatment (i.e., at 120 min for the 7 mW treatment and 6 min for the 150 mW treatment). The tumor treated at 7 mW showed a marked change in T2-weighted contrast evidenced by hypointense regions (*arrow*) in the images compared with pretreatment images (*bottom middle*), indicative of decreased oxygenation and/or acute hemorrhaging. The corresponding tumor response (*right*), assessed 72 h after completion of treatment by injection of Evans blue, confirms exclusion of dye from these tumor regions, indicating shutdown of the vasculature and necrosis. In contrast, T2-weighted images of the tumor treated with 150 mW (*top*) did not reveal changes in SI compared with pretreatment levels. Evans blue staining also showed dye distribution throughout (indicating patent blood supply) at 72 h after treatment and minimal PDT-induced necrosis. Figure 5B shows the onset of PDT-induced changes in oxygenation within the tumor over time for HPPH doses of 3 mg/kg (Fig. 5B, *a*) and 0.1 mg/kg (Fig. 5B, *b*) at the two different power outputs: 150 and 7 mW. False color–coded images of change in SI revealed punctate areas of decreased SI indicative of reduced oxygenation, apparent within 1.5 min of light exposure and increasing over the course of light treatment. The total treatment time for the 150 mW exposures was 6 min (a total energy of 50 J); by the end of which considerably decreased SI (oxygenation) was evident. However, as shown in Fig. 5B, *a* (*top row, far right*) reoxygenation (*blue*) seems to occur after cessation of light at 150 mW. In contrast, a treatment power of 7 mW (Fig. 5B, *a, bottom row*) decreases in

SI is dramatic by ~30 min (a total fluence of only ~13 J), progressively decreasing over time up to 60 min. The patterns observed for the 3 mg/kg HPPH dose are essentially recapitulated at the 0.1 mg/kg HPPH dose (Fig. 5B, *b*).

These observations are supported by the generation of functional T2 activation maps calculated by pixel-by-pixel analysis of statistically significant ($P < 0.05$) change in SI during the course of light treatment compared with pretreatment values (Fig. 6). False color–coded images of changes in SI at the two drug doses are grouped according to the treatment laser power used, 150 mW (Fig. 6A) and 7 mW (Fig. 6B), respectively. Comparison of the images of the 3 mg/kg HPPH dose and an incident power of 150 mW for 5 min (45 J; Fig. 6A, *top left*) with 7 mW for 60 min (25 J; Fig. 6B, *top right*) emphasizes the dramatic differences in tumor oxygenation between the two treatment conditions.

To test whether 150 mW light exposures cause vascular changes that might lead to progressive post-PDT hypoxia, images acquired 10 min after delivery of 45 J were analyzed (Fig. 6A, *right*). As can be seen in T2 activation maps calculated 15 min from the start of light treatment, no such progressive reduction in SI was seen. Analysis of unilluminated control muscle tissue did not show any statistically significant change in SI.

Long-duration light exposure causes pronounced and lasting depression of tumor oxygen levels. Two major mechanisms can account for PDT-induced reductions in tumor oxygenation: photochemical oxygen depletion (14) as computed in Fig. 4B and C and vascular disruption (22). Photochemical oxygen depletion occurs during light exposure of the tissue and is characterized by rapid onset on illumination and equally rapid reversal on cessation of light. Vascular disruption is not instantly reversible, if at all. The persistence of negative BOLD fMRI changes after light exposure suggested that vascular disruption might contribute to treatment outcome and that it might depend on incident laser power. We therefore directly measured tumor oxygen levels before illumination, after various time intervals of illumination, or after completion of illumination, both at high and low laser power and high and low HPPH dose. We first addressed possible acute effects on tumor oxygenation under conditions (3 mg/kg HPPH, 150 mW) for which very high singlet oxygen levels near the vessel wall had been predicted (Fig. 4C, *right*). Tumor pO_2 was measured before and after (light off) just 1 min of illumination at 150 mW. Oxygen levels had decreased sharply (before PDT = 13.7 ± 0.10 mm Hg; after 1-min PDT = 0.85 ± 0.14 mm Hg). The fact that these changes persisted after the light was turned off implies that mechanisms other than photochemical oxygen depletion may be responsible. There was no change observed in tumors of the 0.1 mg/kg HPPH group, consistent with the much lower singlet oxygen levels near the vessel wall predicted for these drug dose conditions. Next, we probed tumor pO_2 after completion of PDT treatment at 0.1 and 3.0 mg/kg HPPH, 100 and 50 J, respectively, at 7 and 150 mW (Fig. 6C). Indicated at the bottom of Fig. 6C are the duration of light exposure and corresponding areas of necrosis achieved in these tumors. In these experiments, the oxygen measurements for the 150 mW short-duration treatments were delayed after completion of light delivery for a period equivalent to the duration of the 7 mW long-duration treatments. This was done to test for possible progression of vascular damage with time following completion of light treatment. It is apparent that both drug dose and duration of light exposure contribute to declines in tumor oxygenation. The extended 7 mW exposures consistently led to greater tumor hypoxia than the short 150 mW treatments. It is evident that, at the end of light exposure, the values for the regimens consisting of 0.1 mg/kg

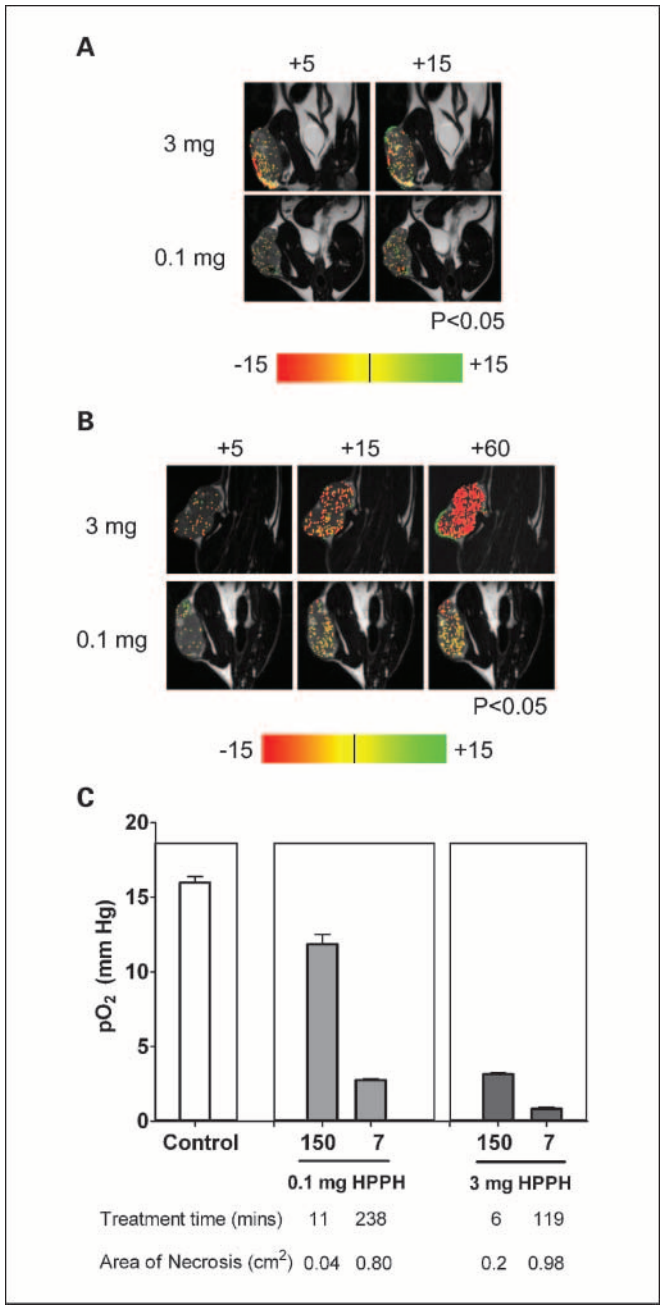

Fig. 6. Functional T2 maps of Ward colorectal carcinomas obtained at different times from the start of light treatment (+5 min, +15 min, and +60 min) following HPPH-PDT at 150 mW (*A*) or 7 mW (*B*). Student's *t* test was done on serially acquired images and pixels within the tumor that showed a statistically significant change ($P < 0.05$) were color coded using a look-up table and reported. HPPH was injected at 3 mg/kg HPPH (*top*) or 0.1 mg/kg HPPH (*bottom*) i.v. ~24 h before light treatment. *C,* measurements of tumor pO_2 in untreated control and HPPH-PDT–treated Ward colorectal carcinomas using the OxyLite system. HPPH was injected at either 0.1 or 3 mg/kg ~24 h before light exposure at 150 or 7 mW. Columns, mean of at least three to four tumors; bars, SE.

HPPH, 150 J, 7 mW and 3 mg/kg HPPH, 50 J, 150 mW are essentially the same (~3 mm Hg); yet, the area of necrosis achieved is 4-fold greater with the first regimen. The difference in outcome can be explained by the fact that hypoxia continues to progress after completion of treatment in the 7 mW regimen, dropping ~10-fold over the next 4 h from 2.76 ± 0.07 mm Hg at the end of 238 min of light to 0.25 ± 0.02 mm Hg ($P < 0.001$). No such progression was observed with the 150 mW regimen.

Discussion

PDT, although used effectively for the treatment of many types of solid tumors, still relies on empirically derived treatment variables that include photosensitizer dose, fluence, and fluence rate. These are usually adjusted so that the duration of patient treatment can be kept short for convenience and patient comfort. However, it has been recognized for some time that the current treatment variables used in clinical settings may not be optimal. For their optimization, a full understanding of the different components that determine PDT dosimetry and effectiveness is necessary. This is a difficult task because of the enormous complexity created by the interplay of the factors that determine tumor destruction and the heterogeneity in the tissue of these factors, especially the availability of oxygen required for the formation of the cytotoxic product. In the present study, we identify the duration of photodynamic exposure, which is a function of fluence rate and fluence, as an important independent factor influencing treatment outcome. Our study further shows that treatment duration affects tumor destruction largely independently of a wide range of photosensitizer doses and fluences (i.e., the drug-light products).

The established benefit of PDT light exposure at low fluence rates in preclinical models has been explained by the conservation of tumor oxygenation during illumination (11, 14, 17), the current paradigm being that high fluence rate leads to photochemical oxygen consumption that overwhelms the oxygen resupply from the microvasculature. Such a mechanism has been proven in preclinical and clinical settings (11, 17, 19, 36, 37). Of particular relevance to our study is a report by Foster et al. (38), which investigated tumor response to various irradiation regimens composed of constant 2-h duration. Fractionated irradiation schedules with dark intervals of 30 to 60 s provided the most durable tumor control, whereas constant irradiance and more rapid fractionation were less efficacious given identical fluences and treatment durations. Because of the existing evidence for photochemical oxygen depletion as a PDT limiting factor, it was the first focus of this study. Simulation of the tumor oxygenation status based on theoretical assumptions for oxygen consumption (14, 31) during light exposure of the tissue predicted extensive oxygen depletion at high fluence rate that was highly photosensitizer concentration dependent. Simulation of the instantaneous singlet oxygen distribution in the tissue emphasized this drug concentration dependence even more. Increasing drug doses should have shifted the fluence rate dependence toward increasingly lower fluence rates for achieving maximum benefit. It was therefore surprising to observe that, in spite of a 30-fold difference in HPPH concentration and 15-fold difference in drug-light product, dependence on the treatment laser power over a range from 3 to 150 mW was strikingly similar.

Although photochemical oxygen depletion is likely to have occurred, neither of the methods we used to determine tumor oxygenation was able to clearly identify its existence. Noninvasive fMRI based on BOLD contrast has previously been used to monitor changes in tumor oxygenation during PDT (39). In the previous study by Gross et al. (39), it was shown that the observed change in BOLD contrast during light treatment was a result of contributions from both photochemical and hemodynamic components. Similarly, in our study, although the use of BOLD fMRI allowed for noninvasive monitoring of changes in oxygenation status during light exposure, it did not distinguish whether these were the consequences of photochemical oxygen depletion or vascular disruption. The direct, invasive oxygen measurements (OxyLite) could only be taken after the light was turned off due to probe limitations and therefore could not determine photochemical oxygen depletion that occurs only during illumination. However, both approaches clearly indicated that acute decreases in tumor oxygenation occurred that were not immediately reversible after cessation of light exposure, indicating that these were not due to purely photochemical processes. Focusing therefore on possible vascular changes, it is noteworthy that, following just 1 min of 150 mW light under conditions of 3 mg/kg HPPH, oxygen measurements closely approached anoxic levels (0.85 ± 0.14 mm Hg). Given the predicted very high singlet oxygen levels near the vessel wall under high-fluence rate conditions (Fig. 4C, *right*), the data suggest acute but transient vascular spasm. The transient nature of this effect is indicated by the eventual recovery of tumor oxygenation observed by BOLD fMRI and the patency of the tumor vasculature to the Evans blue dye delivered 72 h after completion of treatment (Fig. 5A and B). In addition, by 2 h after the end of a 6-min (50 J) treatment, tumor oxygenation was measured at ~3 mm Hg (Fig. 6C), indicating recovery. It is of interest that we have previously observed in a mouse model that normal, but not tumor vasculature, was somewhat protected by brief high-fluence rate PDT using Photofrin (40). This protection could be counteracted by administration of the nitric oxide synthase inhibitor N^{ω}-nitro-L-arginine. These and the current observations may reflect differences in the tumor physiology of the animal models used.

The key finding of this study is the dramatic progression of tumor hypoxia during and after light delivery at low-incident laser power and long duration (Figs. 5 and 6) that is largely independent of drug-light product. We have identified, however, a threshold photosensitizer dose (in this model <0.1 mg/kg) below which even extended illumination fails to elicit any tumor necrosis. Above this dose, the effects of long-duration PDT are striking. As computed in Fig. 4C, extremely low levels of singlet oxygen generated throughout the tissue volume over extended periods of time seem sufficient for tissue destruction. It has to be noted that these computations are based on a theoretical model that assumes optimal conditions for $^1O_2$ production (i.e., optimal vascular supply and drug distribution) and neglect any photobleaching of the photosensitizer during illumination, which might shift oxygenation and therefore $^1O_2$ production to even lower levels. A comprehensive theoretical model describing microscopic dose deposition during PDT, which takes into account temporal and spatial variations in blood flow, oxygen concentration, and photosensitizer distribution, has recently been developed

(15) and could be used in future studies to create more rigorous estimates of photodynamic dose under a wide range of treatment conditions.

The most puzzling result may be found in Fig. 4A and C. Here, it is predicted that the conditions of 0.1 mg/kg HPPH under 150 mW cm^{-2} fluence rate and 3 mg/kg HPPH under 7 mW cm^{-2} fluence rate should produce roughly equal $^1O_2$ amounts and distribution, ranging from ~4 pmol/L at the vessel to ~1 pmol/L at distance. Yet, the actual 150 mW regimen is ineffective, whereas the 7 mW regimen is effective. We propose that the reason for this phenomenon may lie in the intermittent nature of acute hypoxia in tumors. Evidence for fluctuating tumor blood flow has been provided by numerous groups suggesting that tumor blood vessels are often temporarily occluded, resulting in acute hypoxia (41–43). In a previous report by Woodhams et al. (41), it was shown that PDT of normal rat livers using low-power (25 mW) treatment regimen results in a greater reduction in hemoglobin oxygen saturation and increased necrosis compared with high-power illumination (100 mW). Fluorescence angiography measurements showed that the increased necrosis following low-power light treatment was likely due to ischemia/reperfusion injury (41). It is estimated that at least 20% of the surface area of the tumor vasculature is subject to hypoxic changes, which last for at least several minutes (42). Such acute hypoxia would not only protect cells adjacent to the vessels from PDT but also the vasculature itself. This might occur during brief light exposures (such as 5-6 min), and this protection would be largely independent of PDT dose. In contrast, extended light exposures would allow for opening and closing of vessels, thus exposing a much larger fraction of the vasculature to PDT damage, "averaging" the PDT dose over time, and resulting in more effective tumor destruction. The immediate translation of this paradigm faces the significant limitation of prolonged treatment times that are frequently not clinically feasible. It therefore must await the development of novel, possibly portable and/or implantable light sources. Such light sources are currently under development (4).

Disclosure of Potential Conflicts of Interest

No potential conflicts of interest were disclosed.

References

1. Bisland SK, Lilge L, Lin A, Rusnov R, Bogaards A, Wilson BC. Metronomic photodynamic therapy as a new paradigm for photodynamic therapy: rationale and preclinical evaluation of technical feasibility for treating malignant brain tumors. Photochem Photobiol 2004;80:22–30.
2. Boraards A, Varma A, Zhang K, et al. Fluorescence image-guided brain tumour resection with adjuvant metronomic photodynamic therapy: pre-clinical model and technology development. Photochem Photobiol Sci 2005;4:438–42.
3. Henderson BW, Busch TM, Snyder JW. Fluence rate as a modulator of PDT mechanisms. Lasers Surg Med 2006;38:489–93.
4. Lustig RA, Vogl TJ, Fromm D, et al. A multicenter phase I safety study of intratumoral photoactivation of talaporfin sodium in patients with refractory solid tumors. Cancer 2003;98:1767–71.
5. Hall EJ. Radiobiology for the radiologist. Philadelphia: J. B. Lippincott; 1994.
6. Bellnier DA, Lin CW. Photosensitization and split-dose recovery in cultured human urinary bladder carcinoma cells containing nonexchangeable hematoporphyrin derivative. Cancer Res 1985;45:2507–11.
7. Veenhuizen RB, Stewart FA. The importance of fluence rate in photodynamic therapy: is there a parallel with ionizing radiation dose-rate effects? Radiother Oncol 1995;37:131–5.
8. Henderson BW, Gollnick SO. Mechanistic principles of photodynamic therapy. In: Horspool W, Lenci F, editors. CRC handbook of organic photochemistry and photobiology. Boca Raton: CRC Press; 2003. p. 145-1–145-25.
9. Gibson SL, VanDerMeid KR, Murant RS, Raubertas RF, Hilf R. Effects of various photoradiation regimens on the antitumor efficacy of photodynamic therapy for R3230AC mammary carcinomas. Cancer Res 1990; 50:7236–41.
10. Sitnik TM, Henderson BW. Effects of fluence rate on cytotoxicity during photodynamic therapy. In: Dougherty TJ, editor. Optical methods for tumor treatment and detection: mechanisms and techniques in photodynamic therapy VI. Proc SPIE 1997;2972:95–102.
11. Sitnik TM, Hampton JA, Henderson BW. Reduction of tumor oxygenation during and after photodynamic therapy *in vivo*: effects of fluence rate. Br J Cancer 1998;77:1386–94.
12. Angell-Petersen E, Spetalen S, Madsen SJ, et al. Influence of light fluence rate on the effects of photodynamic therapy in an orthotopic rat glioma model. J Neurosurg 2006;104:109–17.
13. Foote CS. Mechanisms of photooxygenation. Prog Clin Biol Res 1984;170:3–18.
14. Foster TH, Murant RS, Bryant RG, Knox RS, Gibson SL, Hilf R. Oxygen consumption and diffusion effects in photodynamic therapy. Radiat Res 1991;126: 296–303.
15. Wang KK, Mitra S, Foster TH. A comprehensive mathematical model of microscopic dose deposition in photodynamic therapy. Med Phys 2007;34: 282–93.
16. Tromberg BJ, Kimel S, Orenstein A, et al. Tumor oxygen tension during photodynamic therapy. J Photochem Photobiol 1990;B5:121–6.
17. Henderson BW, Busch TM, Vaughan LA, et al. Photofrin photodynamic therapy can significantly deplete or preserve oxygenation in human basal cell carcinomas during treatment, depending on fluence rate. Cancer Res 2000;60:525–9.
18. Busch TM, Hahn SM, Evans SM, Koch CJ. Depletion of tumor oxygenation during photodynamic therapy: detection by the hypoxia marker EF3. Cancer Res 2000;60:2636–42.
19. Busch TM, Wileyto EP, Emanuele MJ, et al. Photodynamic therapy creates fluence rate-dependent gradients in the intratumoral spatial distribution of oxygen. Cancer Res 2002;62:7273–9.
20. Georgakoudi I, Foster TH. Singlet oxygen-versus nonsinglet oxygen-mediated mechanisms of sensitizer photobleaching and their effects on photodynamic dosimetry. Photochem Photobiol 1998;67: 612–25.
21. Henderson BW, Fingar VH. Relationship of tumor hypoxia and response to photodynamic treatment in an experimental mouse tumor. Cancer Res 1987;47: 3110–4.
22. Sitnik T, Henderson BW. The effect of fluence rate on tumor and normal tissue responses to photodynamic therapy. Photochem Photobiol 1998;67: 462–6.
23. Takita H, Dougherty TJ. Intracavitary photodynamic therapy for malignant pleural mesothelioma. Semin Surg Oncol 1995;11:368–71.
24. Busch TM, Hahn SM, Wileyto EP, et al. Hypoxia and photofrin uptake in the intraperitoneal carcinomatosis and sarcomatosis of photodynamic therapy patients. Clin Cancer Res 2004;10:4630–8.
25. Bellnier DA, Greco WR, Loewen GM, Nava H, Oseroff AR, Dougherty TJ. Clinical pharmacokinetics of the PDT photosensitizers porfimer sodium (Photofrin), 2-[1-hexyloxyethyl]-2-devinyl pyropheophorbide-a (Photochlor) and 5-ALA-induced protoporphyrin IX. Lasers Surg Med 2006;38:439–44.
26. Cao S, Lu K, Toth K, Slocum HK, Shirasaka T, Rustum YM. Persistent induction of apoptosis and suppression of mitosis as the basis for curative therapy with S-1, an oral 5-fluorouracil prodrug in a colorectal tumor model. Clin Cancer Res 1999;5:267–74.
27. Henderson BW, Bellnier DA, Greco WR, et al. An *in vivo* quantitative structure-activity relationship for a congeneric series of pyropheophorbide derivatives as photosensitizers for photodynamic therapy. Cancer Res 1997;57:4000–7.
28. Pandey RK, Sumlin AB, Constantine S, et al. Alkyl ether analogs of chlorophyll-a derivatives: part 1. Synthesis, photophysical properties and photodynamic efficacy. Photochem Photobiol 1996;64:194–204.
29. Bellnier DA, Henderson BW, Pandey RK, Potter WR, Dougherty TJ. Murine pharmacokinetics and antitumor efficacy of the photodynamic sensitizer 2-[1-hexyloxyethyl]-2-devinyl pyropheophorbide-a. J Photochem Photobiol B Biol 1993;20:55–61.
30. Bellnier DA, Greco WR, Parsons JC, Oseroff AR, Kuebler A, Dougherty TJ. An assay for the quantitation of Photofrin in tissues and fluids. Photochem Photobiol 1997;66:237–44.
31. Henning JP, Fournier RL, Hampton JA. A transient mathematical model of oxygen depletion during photodynamic therapy. Radiat Res 1995;142:221–6.
32. Ogawa S, LeeTM, Nayak AS, Glynn P. Oxygenation-sensitive contrast in magnetic resonance image of rodent brain at high magnetic fields. Magn Reson Med 1990;14:68–78.
33. Young WK, Vojnovic B, Wardman P. Measurement of oxygen tension in tumours by time-resolved fluorescence. Br J Cancer 1996;74:S256–9.
34. Fingar VH, Henderson BW. Drug and light dose dependence of photodynamic therapy: a study of tumor and normal tissue response. Photochem Photobiol 1987;46:837–41.

35. Henderson BW, Gollnick SO, Snyder JW, et al. Choice of oxygen-conserving treatment regimen determines the inflammatory response and outcome of photodynamic therapy of tumors. Cancer Res 2004;64:2120–6.

36. Tromberg BJ, Orenstein A, Kimel S, et al. *In vivo* tumor oxygen tension measurements for the evaluation of the efficiency of photodynamic therapy. Photochem Photobiol 1990;52:375–85.

37. Zilberstein J, Bromberg A, Frantz A, et al. Light-dependent oxygen consumption in bacteriochlorophyll-serine-treated melanoma tumors: on-line determination using a tissue-inserted oxygen microsensor. Photochem Photobiol 1997;65:1012–9.

38. Foster TH, Gibson SL, Gao L, Hilf R. Analysis of photochemical oxygen consumption effects in photodynamic therapy. Proc SPIE 1992;1645: 104–14.

39. Gross S, Gilead A, Scherz A, Neeman M, Salomon Y. Monitoring photodynamic therapy of solid tumors online by BOLD-contrast MRI. Nat Med 2003;9: 1327–31.

40. Henderson BW, Sitnik-Busch TM, Vaughan LA. Potentiation of PDT anti-tumor activity in mice by nitric oxide synthase inhibition is fluence rate dependent. Photochem Photobiol 1999;70:64–71.

41. Woodhams JH, Kunz L, Bown SG, MacRobert AJ. Correlation of real-time hemoglobin oxygen saturation monitoring during photodynamic therapy with microvascular effects and tissue necrosis in normal rat liver. Br J Cancer 2004;91:788–94.

42. Brown JM. Tumor microenvironment and the response to anticancer therapy. Cancer Biol Ther 2002;1:453–8.

43. Chaplin DJ, Olive PL, Durand RE. Intermittent blood flow in a murine tumor: radiobiological effects. Cancer Res 1987;47:597–601.